ARMY RESEARCH LABORATORY

# Synthetic Discriminant Function Performance as a Function of Filter Source Attributes

Michael J. Vrabel

ARL-TN-159 April 2000

**Approved for public release; distribution unlimited.**

20000608 064

The findings in this report are not to be construed as an official Department of the Army position unless so designated by other authorized documents.

Citation of manufacturer's or trade names does not constitute an official endorsement or approval of the use thereof.

Destroy this report when it is no longer needed. Do not return it to the originator.

**Army Research Laboratory**

Adelphi, MD 20783-1197

ARL-TN-159 April 2000

# Synthetic Discriminant Function Performance as a Function of Filter Source Attributes

Michael J. Vrabel

Sensors and Electron Devices Directorate

Sponsored by

AMCOM*

Redstone Arsenal, AL 25898-5240

*Also sponsored by the U.S. Army Research Laboratory.

Approved for public release; distribution unlimited.

## Abstract

The performance of a synthetic discriminant function-based target-detection algorithm is detailed as the filter source attributes are varied to reflect various practical aspects of filter creation.

# Contents





Preceding Page Blank

# Figures

# 1. Introduction

This is the third report in a continuing series of reports [1,2] on the application of the synthetic discriminant function (SDF) approach to automatic target recognition (ATR) (and the exploration of related topics). This report demonstrates the performance of the SDF algorithm in a target-detection mode as the SDF filter image sources progressively transition from ideal sources to those that represent a more real-world scenario. A single filter is used with all SDF models. This use of a single filter is consistent with the optimum performance observed and detailed in the first report [1].

To test the SDF performance, I used the standard scene test set sequence L1816S..._r1.bin. Each of the 236 scenes in this sequence contained two targets: M60 and tnk. For this study, the scenes were treated as if they contained but a single target. That is, if an M60 filter was created, then all scene returns about the location of tnk were suppressed and counted as neither target hits nor background false alarms. In this way, the performance of the SDF model for a comparatively easy-to-detect target (M60) and a much more difficult-to-detect target (tnk) is separately measured. This approach is also consistent with the way one would ultimately like to use the SDF model, the assumption being that it will be used in a comparatively target-poor environment.

# 2. Methodology and Results

As noted in the introduction, this report demonstrates SDF model performance as the filter image source progressively transitions to more realistic sources. Because the SDF model is not scale invariant, scale invariance must be built into the filter. This is done by superimposing target images of varying sizes via the filter creation mechanism. A simple mathematical function has been defined for the 236 scenes of the test set. This function permits a fairly tight square box to be fitted about all targets. The targets can as a consequence be extracted and used as needed for creating filters.

The boxes are also used to define target hits. Two circles are fitted to these boxes: an inner circle (I) just touching the center of each face and an outer circle (O) touching each vertex. (The letters indicated within the parentheses form a simple code for defining test condition attributes when the results are presented.) A target is detected if a hit occurs within one of these circles. As noted in the previous report [1], two options can be used to define the centroid of a potential target hit. The first is to define the hit location as the location of the largest peak response of the SDF model (N) within the area of one of the previously defined circles (discarding all other within-circle peaks). The second is to define the hit location as the peak value weighted average of all hit locations within the circle (Y). Because the previous report [1] indicated that the optimum detection filter count is one, I used only one filter to present the results of this report. Three models are to be used for this study: a baseline, a down-sampled, and an all-aspect model. Each represents a different approach to creating SDF target filters.

## 2.1 Baseline Model

A filter for the baseline model (B) is created from several of the target images contained in the scene set used to test the performance of the SDF algorithm. It is called a baseline model because it can be expected to outperform the remaining two models. This expected performance is a consequence of the unrealistic way the filter is created. Nevertheless, as the model's name implies, it represents a good baseline for comparing the performance of the remaining models.

## 2.2 Down-Sampled Model

As with the baseline model, a filter for the down-sampled model (D) is created from the scene test set. The sequence of test scenes contains targets with a fixed aspect angle but varying range. This is demonstrated in figure 1, a montage of four scenes taken at intervals along the sequence of test images. A single target image, the largest in the test scene sequence, is selected to create the filter. This target image is down sampled to produce a sequence of progressively smaller images spanning the target-size range in the scene set. This sequence of down-sampled images is used to create the filter.

## 2.3 All-Aspect Model

The all-aspect model (A) constructs a filter from representations of all aspect angles of a target. The filter becomes a composite of both these all-aspect angle images and, because scale invariance is required, down-sampled representations of these images. The source of these target images is not the set of test scenes (since, among other reasons, only a single aspect angle is available). The source is an alternate data set available within the

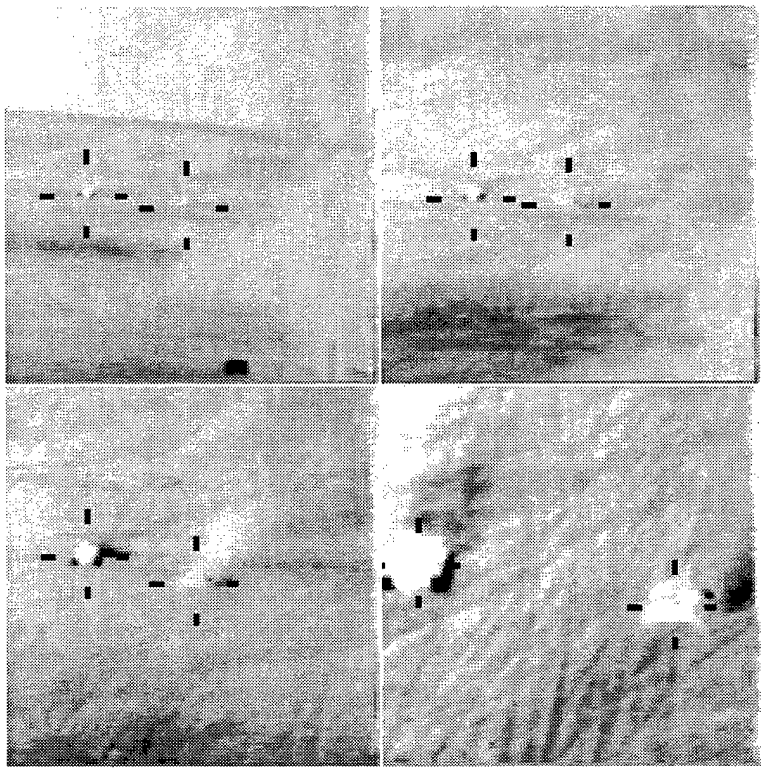

Figure 1. Example scenes with targets indicated by crosshairs.

U.S. Army Research Laboratory (ARL). Although the scene test set contains but a single fixed aspect angle for all targets, the all-aspect model represents the most realistic of the three tests of the SDF algorithm. This is because the all-aspect model most closely represents the manner in which an SDF-based target-detection algorithm is used in a real-world scenario.

## 2.4 Results

In the following subsection, I present the results of the three filter models as a series of target detection versus false alarm curves. The first series is for the baseline model. Figure 2 contains detector performance for the M60 as a function of target filter image count.

The images were taken at uniform intervals along the sequence of 236 scenes. The target image count for the corresponding filter is given in the integer column of the legend. The remaining legend columns are self-explanatory. For the conditions of this test, the optimum filter for the M60 is created from eight target images. The corresponding results for the tnk are also given in figure 2. For the more difficult tnk imagery, the optimum filter is approached more or less asymptotically with increasing target image count.

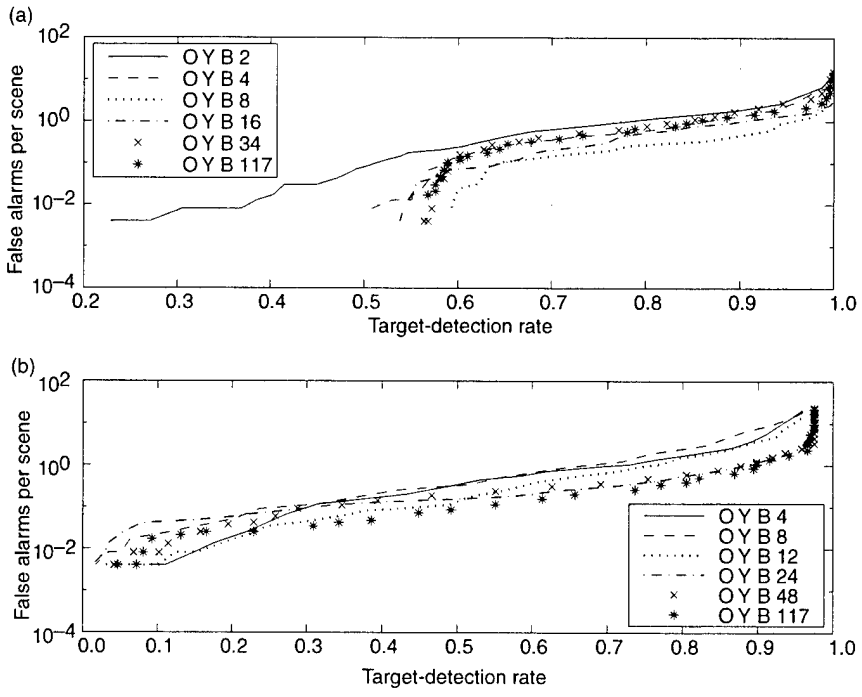


Figure 2. (a) M60 and (b) tnk baseline (B) performance.

O = Outer circle of a target box
Y = Hit location that is average peak value of all hits within circle peak responses

Figure 3 gives the results for the optimum filters of figure 2 as a function of the remaining variables as indicated in the legend.

No clear guideline emerges from this study with regard to the relationship between performance and the variables examined. The results for the down-sampled model are given in figure 4.

Two down-sampled schedules were used. The first schedule produced a sequence of 11 images with each 2 × 2 pixels smaller than the previous image. The second schedule produced a sequence of five images with a 4 × 4 down sample between images. The starting image was number 275, an image near the end of the test sequence. The performance of both the M60 and tnk fell when compared with the baseline models. The performance fall was especially severe for the tnk, where the false-alarm rate increased by an order of magnitude for the same target-detection rate.

To create suitable filters for the all aspect model, I first examined a rather extensive U.S. Army Aviation and Missile Command (AMCOM)-provided image set. The available files are listed in the appendix. This list excludes the standard SDF test sequence. These files contain approximately 30,000

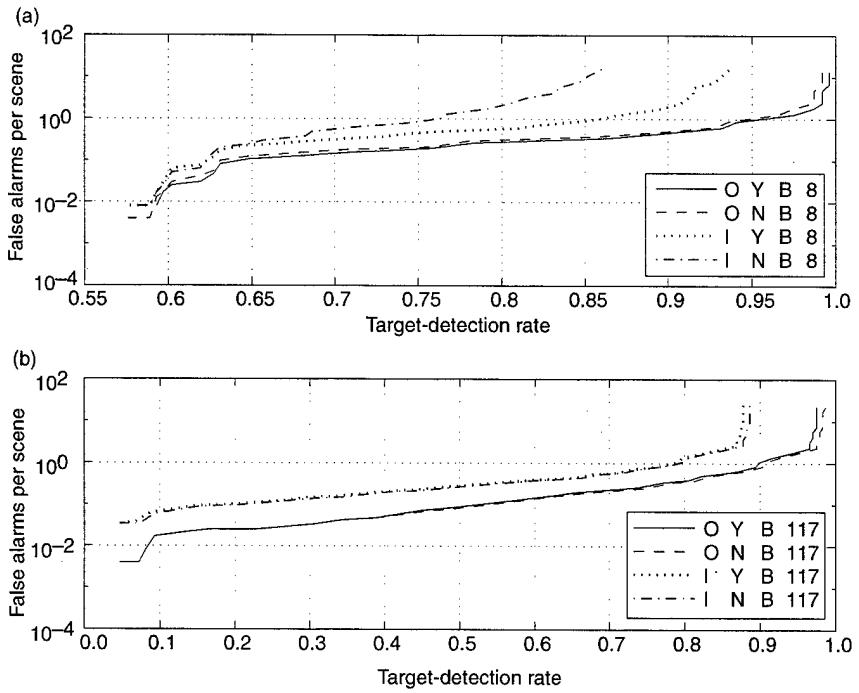


Figure 3. Additional (a) M60 and (b) tnk baseline (B) performance curves.

O = Outer circle of a target box
Y = Hit location that is average peak value of all hits within circle peak responses
I = Inner circle of target box
N = Hit location of largest peak response of SDF model

Figure 4. M60 (lower pair of curves) and tnk down-sampled (D) performance curves.

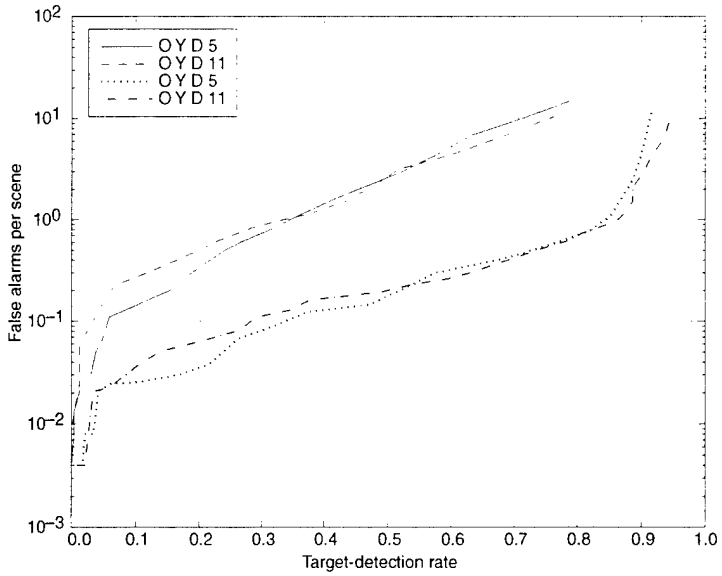


O = Outer circle of a target box
Y = Hit location that is average peak value of all hits within circle peak responses

target-containing scenes. Both the lack of ground-truth data and the quality of the imagery precluded the use of the image set as a filter source.

A second potential all-aspect filter image source (and the one that was used in this study) is a forward-looking infrared (FLIR) database generated by the Army's Night Vision and Electronic Sensors Directorate (NVESD). This database has the desirable attribute that much of the target imagery is available for all aspect angles (at 5° increments). To achieve a best match between the best NVESD M60 and tnk sequences and the AMCOM SDF images, I adjusted the intensity scales, and for the M60, I modified the target images themselves. The resultant NVESD sequences (40 × 75 pixels) are given in figures 5 and 6.

The M60 modifications should be apparent in figure 5. Figure 7 is scene 275 of the SDF test set sequence with the 5° aspect angle NVESD images superimposed (images not to scale).

I performed experiments to find the best down-sampling schedule for the all-aspect model. For the 5° aspect angle M60 image, the following sequence was found to produce the best filter model: 2, 4, 6,. . .28. The numbers refer to the factor by which the $x$ and $y$ pixel count was reduced for the original 40 × 75 windowed image (as given by the first image of figure 5). The same filter sequence was used to produce filters for all the aspect angles of the M60 from 5° through 180°. Each filter was tested on the standard sequence of images (images with an M60 and tnk aspect of about 0° to 5°) with the results of the tests given in figure 8. These curves are the M60

Figure 5. All-aspect-angle sequence of M60: 5° through 180° (40 × 75 pixels).

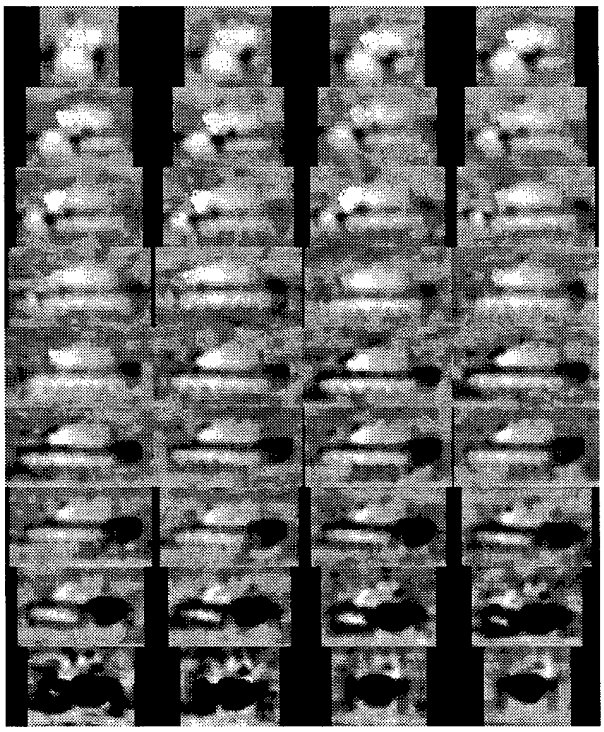

Figure 6. All-aspect-angle sequence of tnk: 5° through 180°.

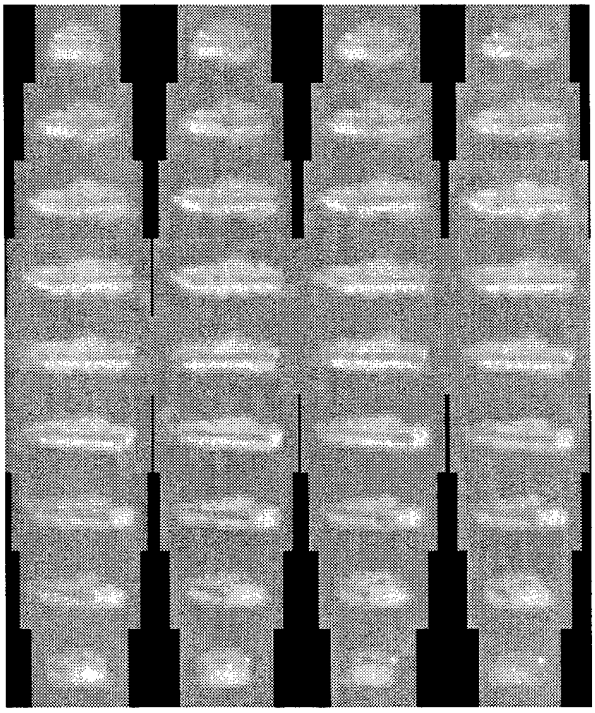

Figure 7. SDF test set sequence scene 275 with superimposed NVESD images.

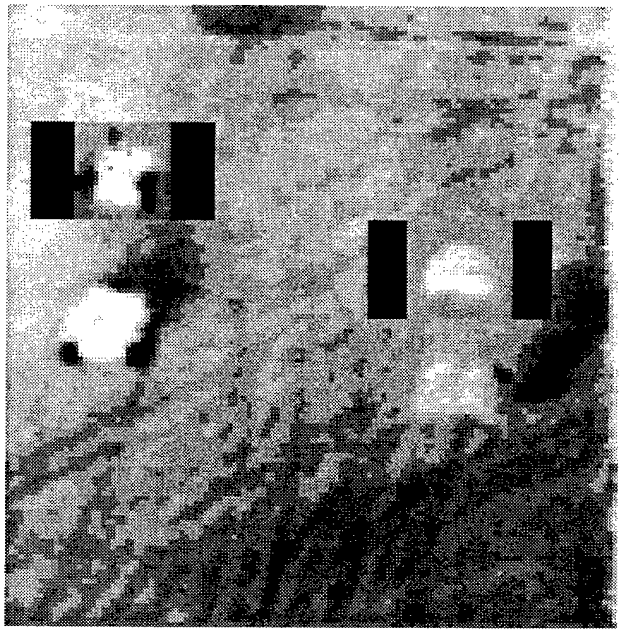

detection rates for average false-alarm rates of 0.5, 1.0, and 2.0. Unexpectedly, the performance of these curves at 180° is better than at 5°. While the 180° view of the M60 has approximately the same silhouette as the front view, the gray-scale appearance of the M60 at 180° does not look like the target presentation in the test scenes. Figure 8 also shows the results for tnk. Despite the seemingly good match at the 0° to 5° aspect angle between the NVESD and AMCOM tnk images, the performance was quite poor.

A final test was performed in which the filter was composed of images at all scales and all aspect angles. Four curves are generated for M60 and tnk. A 360° representation of the images for figures 5 and 6 was created by mirroring of the images below 180°. These images were sampled at 5°, 10°, 20°, and 40° increments. The results are given in figure 9. Because the angular increments show little difference in performance, I did not label the individual curves.

Figure 8. (a) M60 and (b) tnk filter performance as function of filter source aspect angle (A).

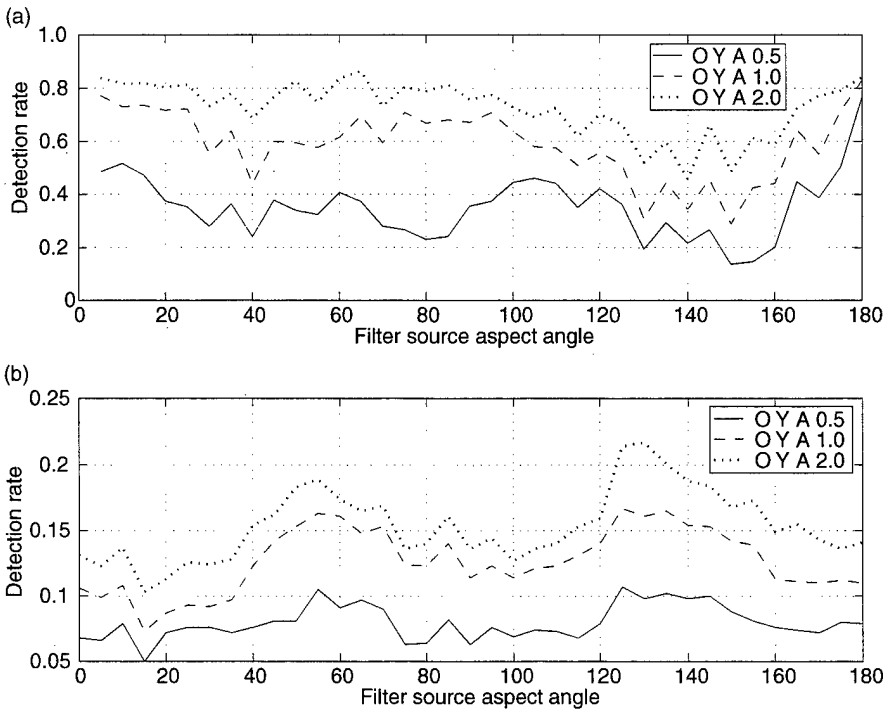


O = Outer circle of a target box
Y = Hit location that is average peak value of all hits within circle peak responses

Figure 9. (a) M60 and (b) tnk filter performance for all scales and all aspect angle.

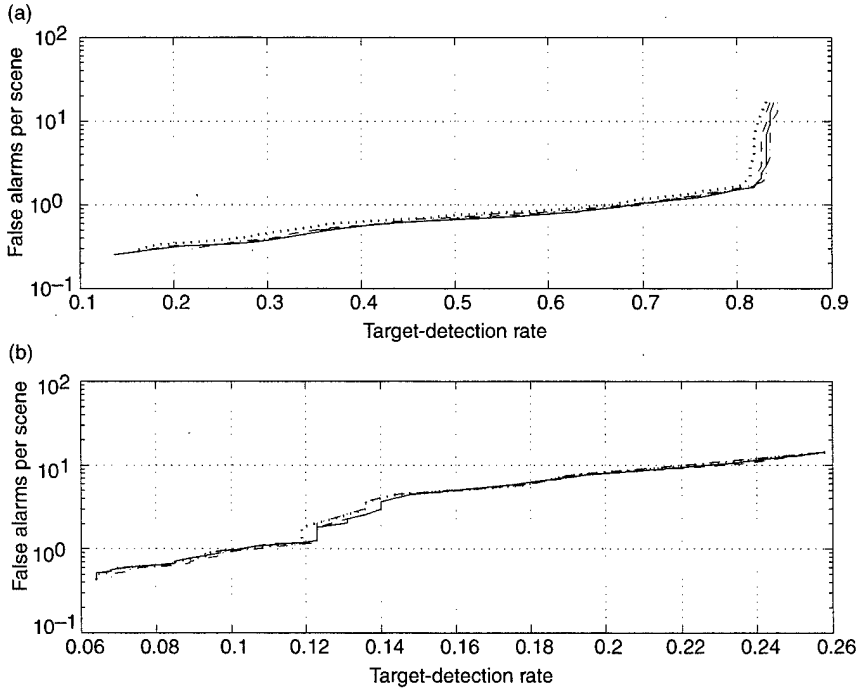

# 3. Conclusion

The performance of an SDF-based target-detection algorithm is examined for a range of filter image sources. Results of a baseline source taken from the algorithm test set are compared with results from sources that represent more of a realistic operational scenario. The results demonstrate the difficulty of maintaining SDF performance as filter sources transition away from unrealistic image sets.

## References


1. M. J. Vrabel, "Synthetic Discriminant Function Performance Versus Filter Count," *U.S. Army Research Laboratory*, ARL-TN-157 (March 2000).

2. M. J. Vrabel, "A Target-Tracking Algorithm," *U.S. Army Research Laboratory*, ARL-TN-158 (March 2000).

# Appendix. AMCOM Image Files and ARL Codes

The list of AMCOM-provided FLIR image sets noted in the main body of the report are given below:

m1_t38_110143_1A040.seqb
m1_t39_110215_1A713.seqb
m3_t13a_072640_4C899.seqb
m3_t14a_072738_4D515.seqb
m3_t15_073100_4F140.seqb
m3_t16_073159_4FDC0.seqb
m3_t16a_073138_4F94E.seqb
m3_t53_061215_232F1.seqb
m3_t56_061130_2294F.seqb
m3_t65_074805_5A12E.seqb
m3_t74_075225_5D89C.seqb
m3_t85_080812_6998D.seqb
m3_t94_080840_69EFC.seqb
m4_144120_5e35.seqb
m4_150426_e8b2.seqb
m5_t11_12_133825_dd50.seqb
m5_t1_132143_2B4D.seqb
m5_t2_132253_3A39.seqb
m5_t3_132446_5251.seqb
m5_t4_132533_5C7B.seqb
m5_t5_132956_70AD.seqb
m5_t6_133054_7D0E.seqb
m5_t7_133335_9F62.seqb
m5_t9_10_133610_C069.seqb
m8_t10_194316_241ED.seqb
m8_t12_194450_25605.seqb
m8_t13_194840_28359.seqb
m8_t14_194920_28C0A.seqb
m8_t16_195040_29D18.seqb
m8_t18_200130.seqb
m8_t19_201932_4019.seqb
m8_t21_202300_6CBD.seqb
m8_t28_204210_1624D.seqb
m8_t29_204250_16AE1.seqb

m8_t8_193833_22256.seqb
m8_t8a_193915_22B5F.seqb
m8_t9_194240.seqb
m8_ta_185500_C4B0.seqb
m8_tb_185540_CD73.seqb
m9_135251_8963.seqb
m9_135600_b5d2.seqb
m9_143026_9b05.seqb

The following is a list of all codes including brief descriptions that I developed for this study (sdf.c: modified*):

aspect_angle.m60.c: Reads one of the outputs of sdf_evaluate.c: results.%d.dat and extracts information for MATLAB plots.

aspect_angle.tnk.c: See aspect_angle.m60.c.

convert.c: Converts the output of montage.c into an sdf.c usable format.

display_file.c: Reads and displays contents of an image file.

display_file1.c: Reads and displays contents of an image file.

filter_cluster.c: Clusters to generate detection filters for use by sdf.c.

filter_cluster1.c: Same as filter_cluster.c but modified to allow code to operate on a subset of the input imagery (see main). This code requires the existence of file: merged_file.

flip_chip.c: Flips 40 × 75 NVESD chips to make a full 360° SDF target presentation.

make_filter_image.c: Creates SDF target filter images from the standard scene test set.

make_frame_list.c: Lists the frames of the standard scene test set for use as test.list by sdf.c (a.out -td 1).

make_list.c: Lists masked target image files for sdf.c detector filter builder.

make_nvl_list.c: Lists test.list for sdf.c from NVESD all aspect angle 40- × 75-pixel images (chips).

make_scene_list.c: Lists (test.list) the SDF test set scenes as input to the filter maker in sdf.c.

montage.c: Creates a montage of sig 40- × 40-chip images for one aspect of M60 or T72 and includes as final image in montage the corresponding SDF target image. Also creates a montage of all aspect angles for a selected NVESD chip. This version is optimized for tnk.

*The original version of sdf.c was written by Lipchen (Alex) Chan of ARL.

montage1.c: Is same as montage.c but optimized for M60.

movie.c: Creates MATLAB-compatible image file to test ground-truth values in movie mode.

movie_maker.c: Reads and displays contents of a file.

plot_maker.c: Creates MATLAB 2-D plots for SDF filter results.

plot_maker1.c: Is same as plot_maker.c but allows a more general labeling of the output legends.

read_file1.c: Reads and displays contents of a file.

read_test.dfil.c: Reads and displays contents of test.dfil.

sdf.c: Is the modified version of sims_sdf.c, the implementation of the SDF-based ATR algorithm.

sdf_evaluate1.c: Evaluates output of sdf.c: detection rate versus false-alarm rate. This version expects the first entry from sdf_output.dat to be scene ID. Scene ID is used to adjust the value of edge to either an inner box circle or an outer box circle.

sdf_imaging.c: Reads and displays in MATLAB format the detector images outputted by sdf.c. Images contain target ground truths. Also has option of reading a set of the original scenes.

template.c: Is a target-tracking code.

temptape.c: Reads and displays contents of an image file.

test_gt.c: Creates a MATLAB-compatible image file to test ground-truth values.

view.c: Views 128 $\times$ 128 SDF scene with superimposed target images.

view_aspect.c: Creates M60 and tnk (5° through 180° aspect angle) image montage.

view_aspect1.c: Creates M60 and tnk (0° through 355° aspect angle) image montage.

Source code listings for these codes are available from the author upon request.

The core codes and their execution sequence for the data generated for the aspect angle models are given below:

- **make_nvl_list.c** $\downarrow$
- **sdf.c** $\rightarrow$ a.out -bd 1 $\downarrow$
- **make_frame_list.c** $\downarrow$
- **sdf.c** $\rightarrow$ a.out -td 1 $\downarrow$
- **sdf_evaluate1.c**

# Distribution

Admnstr
Defns Techl Info Ctr
Attn DTIC-OCP
8725 John J Kingman Rd Ste 0944
FT Belvoir VA 22060-6218

Ofc of the Secy of Defns
Attn ODDRE (R&AT)
The Pentagon
Washington DC 20301-3080

Ofc of the Secy of Defns
Attn OUSD(A&T)/ODDR&E(R) R J Trew
3080 Defense Pentagon
Washington DC 20301-7100

AMCOM MRDEC
Attn AMSMI-RD W C McCorkle
Attn AMSMI-RD-MG-IP R Sims
Redstone Arsenal AL 35898-5240

CECOM
Attn PM GPS COL S Young
FT Monmouth NJ 07703

Dir for MANPRINT
Ofc of the Deputy Chief of Staff for Prsnnl
Attn J Hiller
The Pentagon Rm 2C733
Washington DC 20301-0300

Night Vsn & Elect Sensors Dir
Attn AMSEL-RD-NVOD L Garn
10221 Burbeck Rd Ste 430
FT Belvoir VA 22060-5806

US Army ARDEC
Attn AMSTA-AR-TD M Fisette
Bldg 1
Picatinny Arsenal NJ 07806-5000

US Army Info Sys Engrg Cmnd
Attn ASQB-OTD F Jenia
FT Huachuca AZ 85613-5300

US Army Natick RDEC
Acting Techl Dir
Attn SSCNC-T P Brandler
Natick MA 01760-5002

US Army Simulation, Train, & Instrmntn Cmnd
Attn J Stahl
12350 Research Parkway
Orlando FL 32826-3726

US Army Tank-Automtv Cmnd Rsrch, Dev, & Engrg Ctr
Attn AMSTA-TR J Chapin
Warren MI 48397-5000

US Army Train & Doctrine Cmnd
Battle Lab Integration & Techl Dirctrt
Attn ATCD-B J A Klevecz
FT Monroe VA 23651-5850

US Military Academy
Mathematical Sci Ctr of Excellence
Attn MDN-A LTC M D Phillips
Dept of Mathematical Sci Thayer Hall
West Point NY 10996-1786

Nav Surface Warfare Ctr
Attn Code B07 J Pennella
17320 Dahlgren Rd Bldg 1470 Rm 1101
Dahlgren VA 22448-5100

DARPA
Attn S Welby
3701 N Fairfax Dr
Arlington VA 22203-1714

Hicks & Associates Inc
Attn G Singley III
1710 Goodrich Dr Ste 1300
McLean VA 22102

Palisades Inst for Rsrch Svc Inc
Attn E Carr
1745 Jefferson Davis Hwy Ste 500
Arlington VA 22202-3402

US Army Rsrch Ofc
Attn AMSRL-RO-D JCI Chang
Attn AMSRL-RO-EN W Bach
PO Box 12211
Research Triangle Park NC 27709

## Distribution (cont'd)

US Army Soldier & Biol Chem Cmnd Dir of
Rsrch & Techlgy Dirctrt
Attn SMCCR-RS I G Resnick
Aberdeen Proving Ground MD 21010-5423

TECOM
Attn AMSTE-CL
Aberdeen Proving Ground MD 21005-5057

US Army Rsrch Lab
Attn AMSRL-DD J M Miller
Attn AMSRL-CI-AI-A Mail & Records Mgmt

US Army Rsrch Lab (cont'd)
Attn AMSRL-CI-AP Techl Pub (3 copies)
Attn AMSRL-CI-LL Techl Lib (3 copies)
Attn AMSRL-IS-EP P Gillespie
Attn AMSRL-SE J Pellegrino
Attn AMSRL-SE-SA J Eicke
Attn AMSRL-SE-SE M Vrabel (5 copies)
Adelphi MD 20783-1197

# REPORT DOCUMENTATION PAGE

*Form Approved*
*OMB No. 0704-0188*

Public reporting burden for this collection of information is estimated to average 1 hour per response, including the time for reviewing instructions, searching existing data sources, gathering and maintaining the data needed, and completing and reviewing the collection of information. Send comments regarding this burden estimate or any other aspect of this collection of information, including suggestions for reducing this burden, to Washington Headquarters Services, Directorate for Information Operations and Reports, 1215 Jefferson Davis Highway, Suite 1204, Arlington, VA 22202-4302, and to the Office of Management and Budget, Paperwork Reduction Project (0704-0188), Washington, DC 20503.

| 1. AGENCY USE ONLY *(Leave blank)* | 2. REPORT DATE | 3. REPORT TYPE AND DATES COVERED |
|---|---|---|
| | April 2000 | Final, 1 Oct 98 to 30 Sept 99 |

**4. TITLE AND SUBTITLE** Synthetic Discriminant Function Performance as a Function of Filter Source Attributes

**5. FUNDING NUMBERS**
DA PR: AH16
PE: 62120A

**6. AUTHOR(S)** Michael J. Vrabel

**7. PERFORMING ORGANIZATION NAME(S) AND ADDRESS(ES)**
U.S. Army Research Laboratory
Attn: AMSRL-SE-SE email: vrabel@arl.mil
2800 Powder Mill Road
Adelphi, MD 20783-1197

**8. PERFORMING ORGANIZATION REPORT NUMBER**
ARL-TN-159

**9. SPONSORING/MONITORING AGENCY NAME(S) AND ADDRESS(ES)**
AMCOM*
Redstone Arsenal, AL 25898-5240

**10. SPONSORING/MONITORING AGENCY REPORT NUMBER**

**11. SUPPLEMENTARY NOTES**
ARL PR: 9NE4MM
AMS code: 622120.H16
*Also sponsored by the U.S. Army Research Laboratory.

**12a. DISTRIBUTION/AVAILABILITY STATEMENT**
Approved for public release; distribution unlimited.

**12b. DISTRIBUTION CODE**

**13. ABSTRACT** *(Maximum 200 words)*
The performance of a synthetic discriminant function-based target-detection algorithm is detailed as the filter source attributes are varied to reflect various practical aspects of filter creation.

**14. SUBJECT TERMS**
Target tracking, automatic target recognition, template matching, correlation filters, SDF

**15. NUMBER OF PAGES**
24

**16. PRICE CODE**

| 17. SECURITY CLASSIFICATION OF REPORT | 18. SECURITY CLASSIFICATION OF THIS PAGE | 19. SECURITY CLASSIFICATION OF ABSTRACT | 20. LIMITATION OF ABSTRACT |
|---|---|---|---|
| Unclassified | Unclassified | Unclassified | UL |

NSN 7540-01-280-5500

Standard Form 298 (Rev. 2-89)
Prescribed by ANSI Std. Z39-18
298-102